Sensors and Materials, Vol. 19, No. 8 (2007) 477–485
MYU Tokyo

S & M 0698

Fabrication of High-Q FBAR with Mesa-Shaped Membrane Structure

Hae-Seok Park*, Jooho Lee, Kwang Jae Shin[1],
Sang Hun Lee and Insang Song

Samsung Advanced Institute of Technology, Suwon-Si, Gyounggi-Do, P.O. Box 111, Korea
[1]MEMS Solution, Yongin-Si, Gyounggi-Do, P.O. Box 25, Korea

(Received May 8, 2007; accpeted September 7, 2007)

Key words: bulk acoustic wave device, piezoelectric resonator filter

In this paper, we present a newly developed high-Q film bulk acoustic resonator (FBAR), which has a piezoelectric AlN film sandwiched between two electrode films and a mesa-shaped membrane structure by utilizing polysilicon and XeF_2 as a sacrificial layer and dry release gas, respectively. By controlling the etching profile of the bottom-electrode and the sacrificial layers, the growth of a poorly formed AlN layer at the edge of the mesa-shaped membrane could be eliminated. Moreover, by optimizing the space between the sacrificial layer and the top/bottom-electrode layer, we could improve the characteristics of the resonator and filter. When we compare our new FBAR with a typical surface-micromachined FBAR, such as a resonator having its own Bragg reflector or cavity, we can greatly reduce the need for the tight control of chemical mechanical polishing (CMP) of the layer underneath the resonator. The measured Q value and the effective electromechanical coupling coefficient of the resonator with an area of 120×120 μm^2 were 1450 and 6.43%, respectively. The peak insertion loss (IL) and the bandwidth of the filter were 0.60 dB and 70 MHz, respectively.

1. Introduction

Recently, there has been strong demand for the faster evolution of RF components because of the rapidly increasing market for wireless devices.[1] In particular, miniaturization and multifunctionality in mobile handsets are required with the increase in operating frequencies. These trends have resulted in RF components including filters having a smaller size as well as higher performance.[2,3] Typical commercialized filters used in the RF front-end for wireless handsets are ceramic or surface acoustic wave (SAW) filters.[4] However, it has been revealed that these filters have inherent difficulties in the

*Corresponding author: e-mail: hspark71@samsung.com

implementation of miniaturized on-chip systems. Also, SAW filter technology is likely to become inadequate for high-frequency applications due to high insertion loss and fabrication difficulties. Film bulk acoustic resonators (FBARs) are electromechanical resonators that use electroacoustic resonance rather than electromagnetic (EM) resonance. This makes FBARs considerably smaller than EM-based resonators because the wavelengths of acoustic waves are about five orders of magnitude shorter than those of electromagnetic waves. FBAR filters are not only characterized by their small dimensions but also by their low losses and high-power handling capabilities.[5] In this work, we fabricate a piezoelectric resonating device with high performance that can be readily formed on an integrated circuit substrate without damage to other circuit elements.

2. Design

In this paper, we propose a newly developed high-Q FBAR with a mesa-shaped membrane. Schematic diagrams of the proposed structure and the conventional structure with a cavity are shown in Fig. 1. Using a mesa-shaped membrane structure, we can reduce the need for the tight control of chemical mechanical polishing (CMP) of the layer underneath the resonator, which is required in the fabrication of typical FBAR filters. Also, a long etching time for the removal of the silicon substrate is not required due to the formation of a resonating thin film over the air gap. Consequently, the time required for the production process may be greatly reduced and other integrated circuits may be easily assembled on the same substrate.

In general, an FBAR is preferably formed by placing the step edge of the bottom electrode and the piezoelectric material away from the unsupported region (air gap) to increase its strength and ensure that it is able to withstand a wide range of stress. However, our proposed structure has a lower coupling coefficient and Q factor due to the parasitic overlap in which both of the electrodes and the piezoelectric layer reside directly on the substrate. To reduce this problem, we evaluated the characteristics of the resonators by varying space **a** between the sacrificial layer and the top-electrode layer and by varying space **b** between the sacrificial layer and the bottom-electrode layer, as shown in Fig. 1(b). On the basis of these results, we fabricated and evaluated the FBAR resonator and filter.

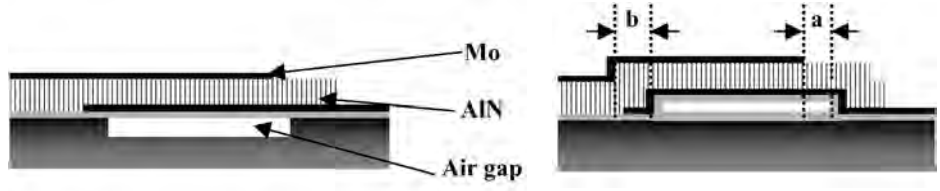

(a) (b)

Fig. 1. (a) Conventional FBAR structure with cavity. (b) Proposed FBAR structure with mesa-shaped membrane. Schematic diagrams of FBARs.

3. Fabrication

We used aluminum nitride (AlN), molybdenum (Mo) and silicon nitride (SiNx) as piezoelectric, top/bottom-electrode and membrane materials, respectively.

The detailed fabrication process is shown in Fig. 2. A silicon dioxide layer for protecting the silicon substrate from XeF_2 gas and a polysilicon layer as a sacrificial layer

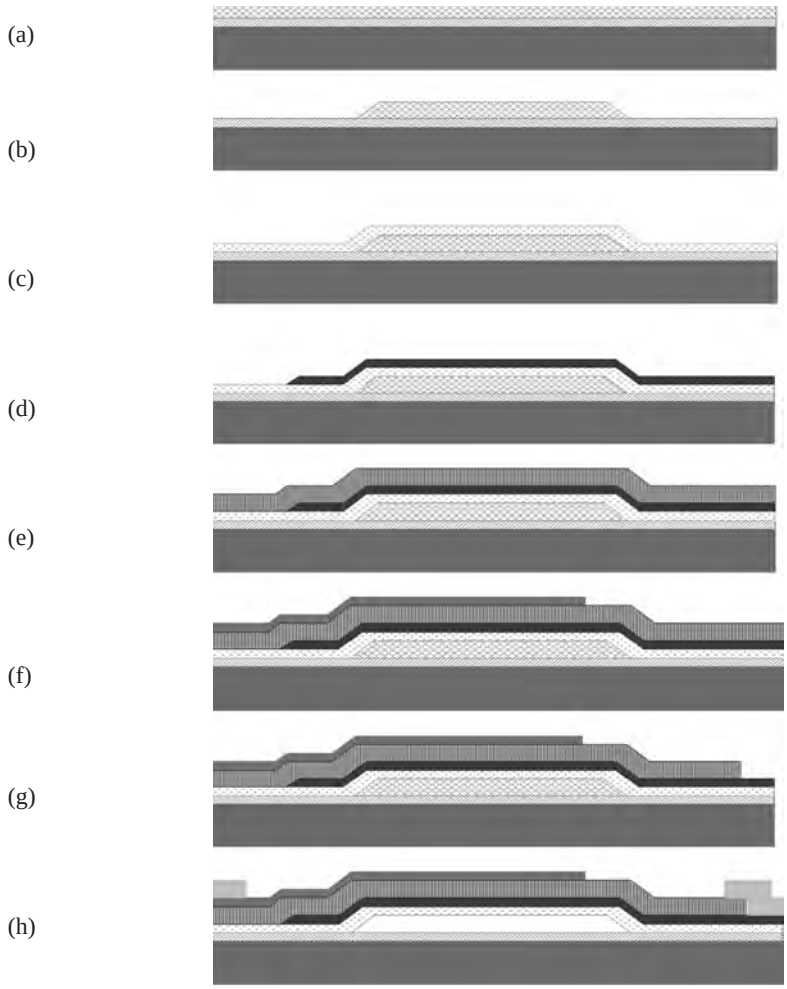

Fig. 2. (a) SiO_2 and polysilicon layer deposition. (b) Polysilicon layer etching. (c) Membrane-layer deposition. (d) Bottom-electrode-layer deposition and etching. (e) Piezoelectric-layer deposition. (f) Top-electrode layer deposition and etching. (g) Piezoelectric-layer etching. (h) Pad-layer liftoff and removal of polysilicon layer. Fabrication process of FBAR with mesa-shaped membrane.

were deposited by thermal wet oxidation and low-pressure chemical vapor deposition (LPCVD), respectively, as shown in Fig. 2(a). After etching the polysilicon layer by reactive ion etching (RIE), silicon nitride as a membrane layer was deposited and a Mo layer as a bottom electrode was deposited and patterned [Figs. 2(b)–2(d)]. To suppress the growth of a poorly formed AlN layer around the edge of the mesa-shaped membrane and bottom electrode, it is essential to make the etching profile correctly inclined. Figures 2(e) and 2(f) show the deposition of the AlN layer as a piezoelectric layer and the patterning of a Mo layer as a top-electrode layer, respectively. Since an FBAR is a thickness-mode resonator, AlN should be well oriented along the c-axis. To connect the top and bottom electrodes to the pad, the AlN layer was etched by inductively coupled plasma (ICP) RIE and then the pad layer was patterned by the liftoff process. Then a dry release process using XeF_2 was applied to remove the sacrificial polysilicon layer to form a freestanding resonator, as shown in Figs. 2(g) and 2(h).

4. Results and Discussion

AlN layers must be grown oriented in the (002) direction to achieve high piezoelectric coupling to the required extensional mode. Therefore, columnar AlN grains whose c-axes are perpendicular to the substrate are required. A cross-sectional SEM image of the densely packed columnar AlN structure is shown in Fig. 3(a). Because of the strong dependence of the film texture on the coupling coefficient, it is necessary to have a rocking curve with a small full width at half maximum (FWHM) to achieve a high electromechanical coefficient. The wide-angle curves and rocking curves are shown in Figure 3(b), and the measured FWHM of the AlN structure was 1.90°.

To obtain improved characteristics of the FBAR, suppressing the poorly grown columnar piezoelectric layer around the edge of the bottom layer is important so as to avoid its undesirable scattering effect. In our mesa-shaped membrane structure, poorly formed AlN is grown at the edge of the sacrificial and bottom-electrode layers if they have a steep etching profile. To control the etching profile of the polysilicon layer, we change the ratio of the etching gas (SF_6/O_2) from 0.5 to 0.9 while using the same total amount of gas of 170 sccm. Figures 4(a)–4(c) show cross-sectional SEM images of the AlN grown at gas ratios of 0.5, 0.7 and 0.9, respectively. As shown in these figures, the quality of the AlN layer deteriorates as the etching profile becomes steeper [Fig. 4(a)]. In addition, by changing the ratio of the etching gas for the bottom electrode (SF_6/O_2) from 2.0 to 5.0, a suitable etching profile for achieving a well-grown AlN layer at the edge of the bottom electrode was obtained, as shown in Fig. 5. Under the consideration of AlN growth and the critical dimension loss, we chose SF_6/O_2 ratios of 0.7 and 5.0 for the etching conditions of the sacrificial and bottom-electrode layers, respectively. The results of fabrication and the characteristics of FBARs with poorly grown and well-grown AlN are compared in Fig. 6. Microcracks and the nonconformal deposition of the top electrode on the AlN layer result from the poorly grown AlN [Fig. 6(a)]. These defects have great potential for causing various problems: disconnection in the electrode, nonuniform thickness of the top electrode and poor reliability. Figure 6(c) shows the characteristics of the FBARs with different AlN structures. Dotted and solid lines in this

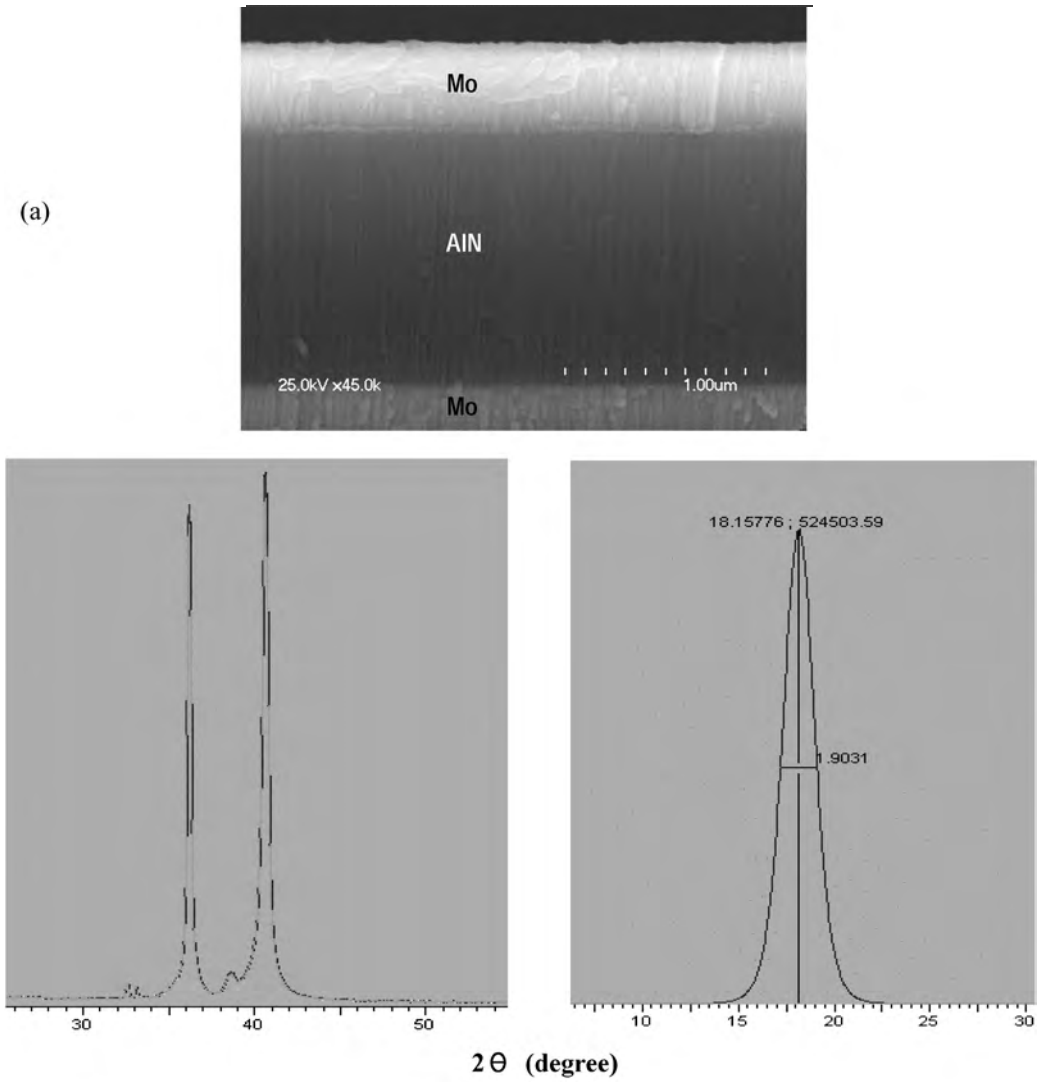

(b)

Fig. 3. (a) Cross-sectional SEM image of Mo /AlN/ Mo layer. (b) Wide-angle curves and rocking curves of AlN layer deposited on Mo / Si wafer. Characteristics of columnar AlN grains with c-axis perpendicular to substrate.

figure represent the S-parameter responses of the FBAR with poorly grown and well-grown AlN, respectively. The degradation of the insertion loss and rejection level in the FBAR with poorly grown AlN can be seen in this figure in comparison with the FBAR with well-grown AlN.

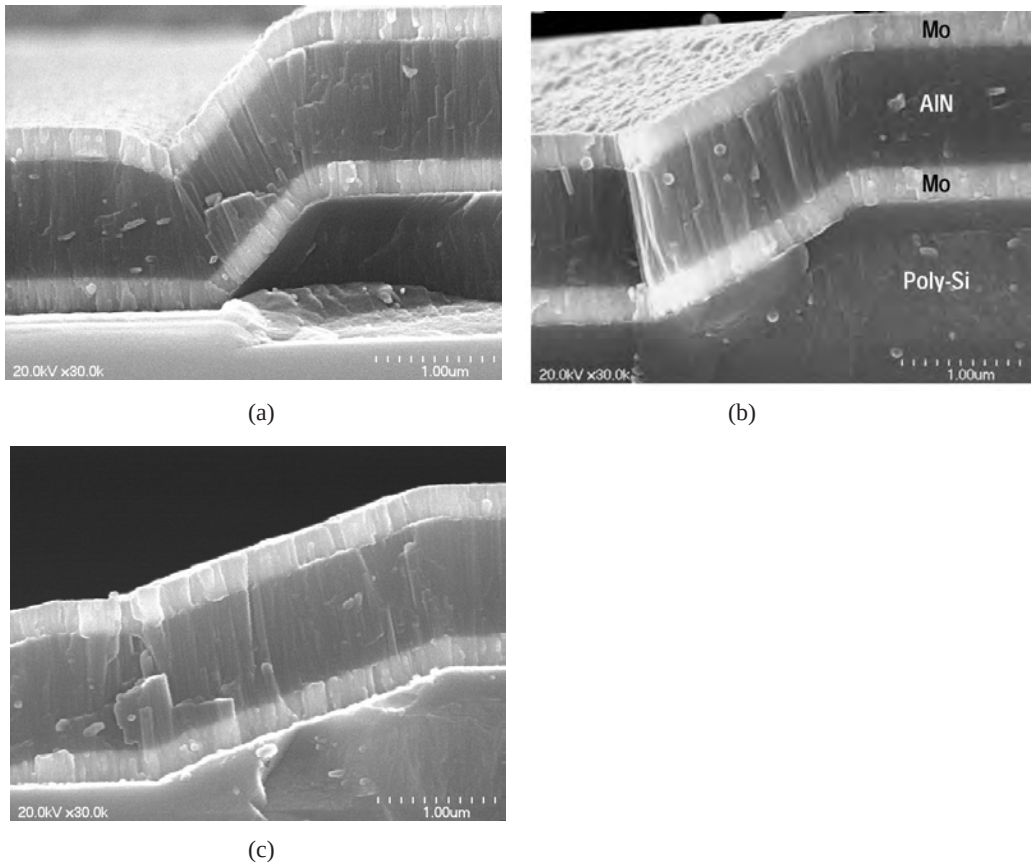

Fig. 4. AlN growth with change in etching profile of poly-Si layer.

As mentioned above, our FBAR, which is formed by placing the step edge of the bottom electrode and the piezoelectric material away from the unsupported region, has a lower coupling coefficient and Q factor due to the parasitic overlap in which both of the electrodes and the piezoelectric layer reside directly on the substrate. To reduce this problem, we vary space **a** between the sacrificial layer and the top-electrode layer from –6 to 6 μm (minus and plus mean that the top-electrode layer is located inside and outside the sacrificial layer, respectively) and vary space **b** between the sacrificial layer and the bottom-electrode layer (2, 4 and 6 μm), as shown in Fig. 1(b).

The quality factor of the resonators is decreased markedly when the top electrode expands over the sacrificial layer, and the electromechanical coupling coefficient of the resonators decreases with increasing space between the sacrificial and bottom layers, as shown in Fig. 7. On the basis of this, we fabricated a resonator and filter with $a = -4$ μm and $b = 2$μm. To analyze the fabricated FBAR filter, measurement is performed using an 8510C vector network analyzer, a 250-μm-pitch coplanar GGB picoprobe, and a GGB CS-5 SOLT calibration standard. The S_{11} and S_{12} parameters of the resonator are shown

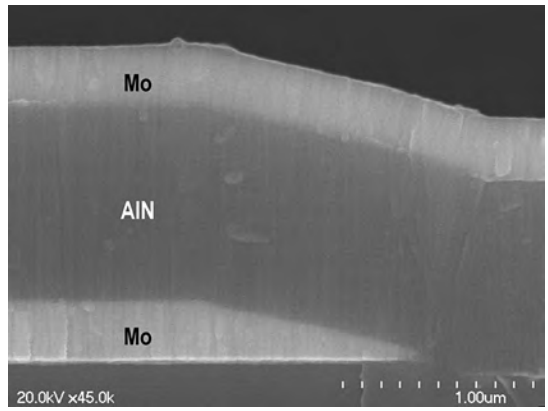

Fig. 5. Cross-sectional SEM image of edge of bottom electrode.

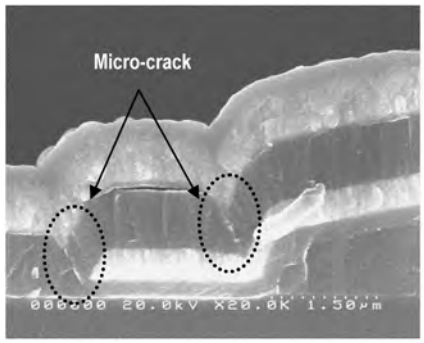

(a)

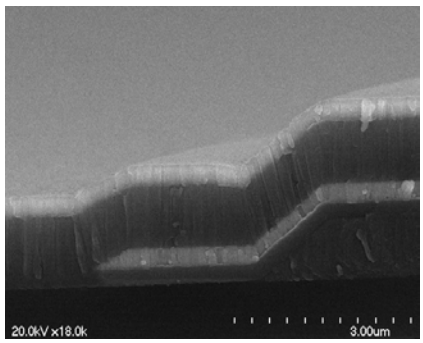

(b)

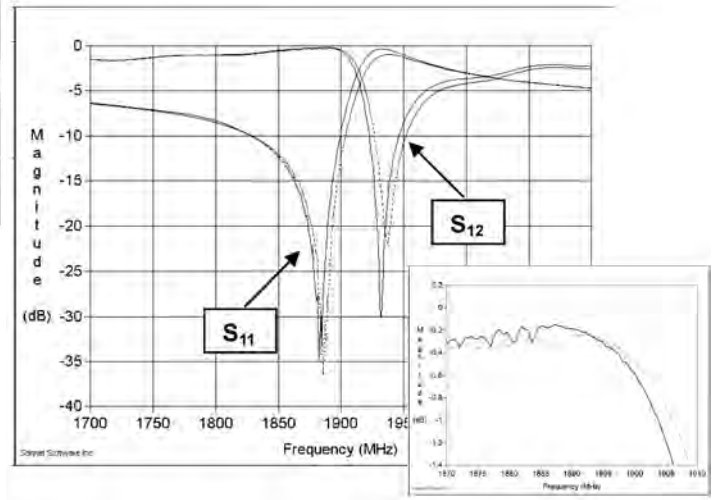

(c)

Fig. 6. (a) Cross-sectional SEM image of FBAR with poorly grown AlN. (b) Cross-sectional SEM image of FBAR with well-grown AlN. (c) Comparison of characteristics of FBAR with poorly grown and well-grown AlN (dotted line: FBAR with poorly grown AlN, solid line: FBAR with well-grown AlN). Fabrication results and characteristics of FBAR with poorly grown and well-grown AlN.

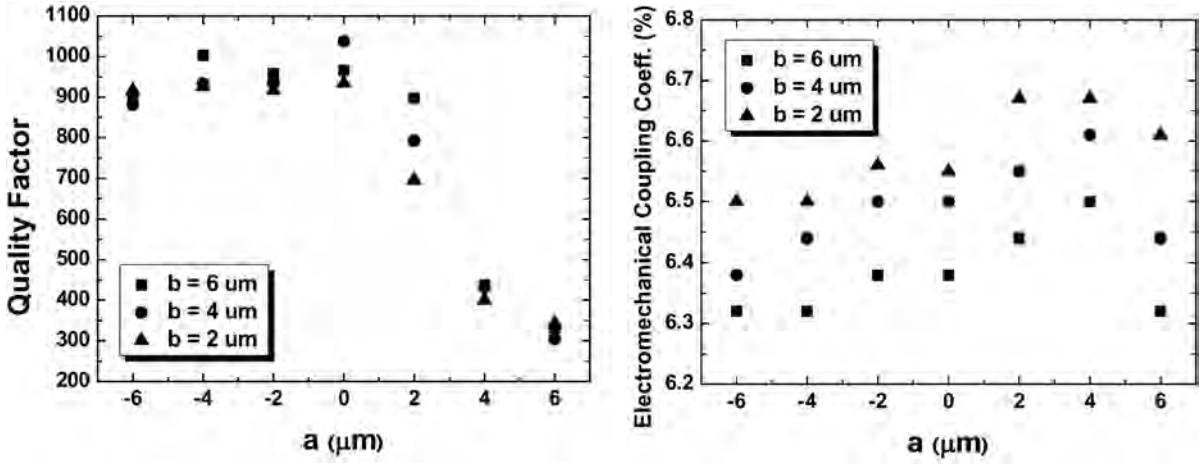

(a) (b)

Fig. 7. (a) Quality factor of resonators with the area of 120×120 μm². (b) Effective electromechanical coupling coefficient of resonators. Characteristics of resonators.

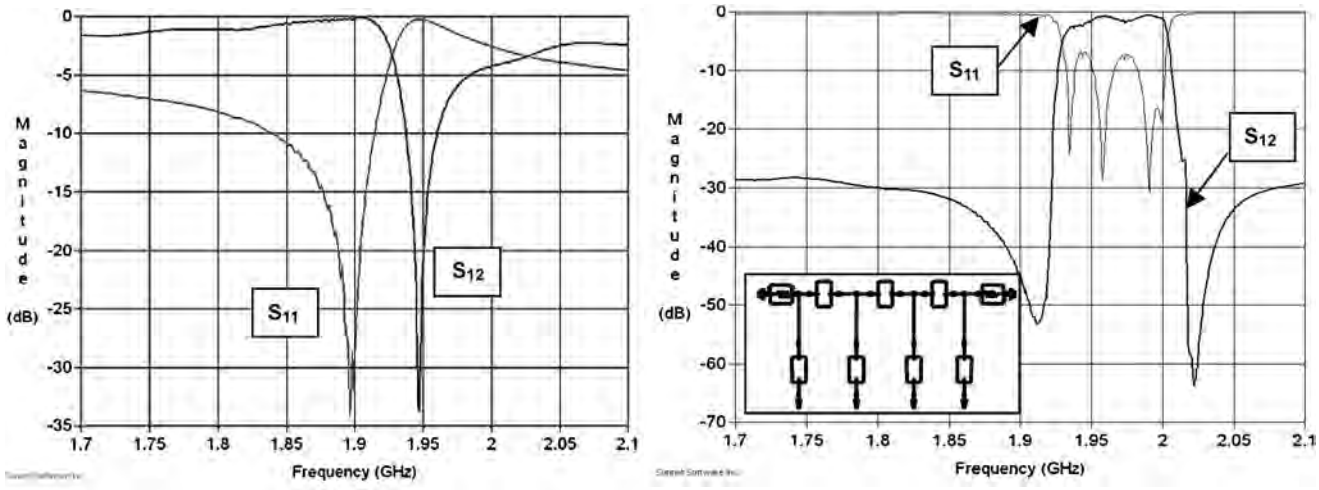

(a) (b)

Fig. 8. S-parameter response of (a) fabricated resonator (area: 120×120 μm²) and (b) filter (fine line: S_{11} response, thick line: S_{12} response).

in Fig. 8(a) and those of the filter with the FBAR topology are shown in Fig. 8(b). In this figure, the thick line represents the S_{12} response. In the resonator with an area of 120 ×120 μm² and where **a** and **b** are –4 and 2 μm, respectively, the measured Q value was

1450 and the effective electromechanical coupling coefficient was 6.43%. The fabricated filter has a minimum insertion loss (IL) of 0.6 dB and a bandwidth of 70 MHz.

5. Conclusions

In this work, an RF filter composed of an FBAR with a mesa-shaped membrane was investigated. To fabricate a resonator with high performance and reliability, we controlled the etching profile of the sacrificial and bottom-electrode layers. As a result, the growth of a poorly formed AlN layer at the edge of the mesa-shaped membrane could be eliminated. In addition, the coupling coefficient and quality factor of the resonator could be controlled individually by changing the space between the sacrificial layer and the top/bottom electrode without modifying the AlN layer. On the basis of this result, we fabricated a high-performance resonator and filter. The measured Q value and the effective electromechanical coupling coefficient of the resonator with an area of 120× 120 μm^2 were 1450 and 6.43%, respectively. The peak IL and the bandwidth of the filter were 0.60 dB and 70 MHz, respectively. Through the development of the mesa-shaped FBAR, we can still apply core technologies for the integration of FBARs with other RF components. Furthermore, this development will create and capture new markets for RF FBAR applications.

References

1 R. Ruby, P. Bradley, Y. Oshmyansky, A. Chien and J. D. Larson III: IEEE Ultrasonics Symp., 2001 (Atlanta, 2001) p. 813.
2 T. L. Ren, Y. X. Liu, J. S. Liu, L. T. Liu and S. J. Li: Proc. 6th Int. Conf. Solid-State and Integrated-Circuit Technology (Shanghai, 2001) p. 726.
3 K. W. Kim, J. G. Yook, M. G. Gu, M. Y. Song, Y. J. Yoon and H. K. Park: IEEE MTT-s Digest (Seatle, 2002) p. 1181.
4 M. Kikita, N. Shibagaki, T. Akagi and K. Sakiyama: IEEE Ultrasonics Symp. (Baltimore, 1993) p. 15.
5 O. Ikata, N. Nishihara, Y. Satoh, H. Fukushima and N. Hirisawa: IEEE Ultrasonics Symp. (Lake Tahoe, 1999) p. 2257.